

Methylated Tetrahydrophthalic Anhydrides as End Caps in Addition Polyimides

David E. Rajsfus,[†] Mary Ann B. Meador,[‡] and Aryeh A. Frimer^{*,†}

[†]Ethel and David Resnick Chair in Active Oxygen Chemistry, Bar-Ilan University, Ramat Gan 52900, Israel, and [‡]NASA Glenn Research Center, Cleveland, Ohio 44135

Received May 3, 2010; Revised Manuscript Received June 7, 2010

ABSTRACT: Thermolysis of methylenedianiline (MDA) 1,2,3,6-tetrahydrophthalic (THP) bismides up to 371 °C, produces aromatic product, with a concomitant lowering in cross-linking. This aromatization is responsible for both the improved thermal oxidative stability of THP end-capped polyimides and their substantial frangibility. In the hope of inhibiting precuring aromatization, 2,3-dimethyl, 3,3-dimethyl, and 1,2,3-trimethyl THP analogues were synthesized and reacted with MDA in a 2:1 ratio, heating gradually from 204 to 371 °C. In the lower temperature range, monoimide transforms to bisimide. At temperatures above 320 °C, cross-linking predominates—generally reaching ~30% at 371 °C, though it was as much as 69% for 3,3-dimethyl THP. The surprising facility of cross-linking in the latter was correlated to the double bond length of the *trans* imide formed via thermal enolization. The aromatization (2–25%) observed in these methylated systems at higher temperatures presumably results from oxidative decarboxylation of the pendant methyls, which is the preferred pathway for degradation after cross-linking.

Introduction

PMR polyimide resins^{1,2} are polymers conveniently prepared from monomeric reagents (hence, the acronym PMR) which are widely used as polymer matrix composite materials for aircraft engine applications. They combine ease of processing with good oxidative stability up to 300 °C.³ PMR polyimides, commonly used in the aerospace industry, are generally capped at each end by a dicarboxynorbornenyl (nadic) moiety. This end-cap serves a double function: (1) the dicarboxy functionality limits the number of repeating units and, hence, the average molecular weight of the various polymer chains (oligomers), thereby improving processability; (2) upon further thermal treatment (curing), the pinched olefinic linkage of the nadic end-cap cross-links the various oligomer strands into a low density, high specific strength, tough heat-resistant piece. The mechanism of this cross-linking was elegantly elucidated in 1997 by Meador and co-workers.⁴ Figure 1 outlines the preparation of PMR-15 (molecular weight 15 000 amu; $n = 2.084$) from methylenedianiline (MDA), benzophenonetetracarboxylic diacid diester (BTDE), and nadic acid ester (NE).⁵

Paradoxically, however, recent research has shown that it is this very end-cap, so important to processing, that accounts for much of the weight loss in the polymer on aging in air at elevated temperatures (>315 °C).⁴ Over the past decade, we have explored various aspects of this thermo-oxidative degradation in the hope of gleaning clues on how to design new end-caps which will slow down this degradation, and prolong the use lifetime of polyimide materials. Several years ago, we reported a number of studies on the thermo-oxidative aging of a modification of PMR-15, in which we ¹³C-labeled the norbornenyl end-cap at the methyne carbon α to the carbonyl groups.^{4,6,7} On the basis of this work, it was concluded that this oxidation proceeds through the two primary pathways shown in Figure 2.

Path A degradation proceeds through initial cleavage of the norbornyl ring to form a biradical which undergoes attack of oxygen to form a 2-hydroxy substituted maleimide **2**. Such cleavage products are most likely formed concomitant with large amounts of weight loss in the polymer system.

Path B degradation, on the other hand, proceeds through oxidation of the bridging methylene of the norbornene moieties followed by carbon monoxide extrusion. Aromatization of the intermediate biradical leads to substituted quinone **3** or phthalimide **4**, and related secondary degradation products. Such structures are formed with very little weight loss. Therefore, new end-cap structures that more strongly favor path B degradation should

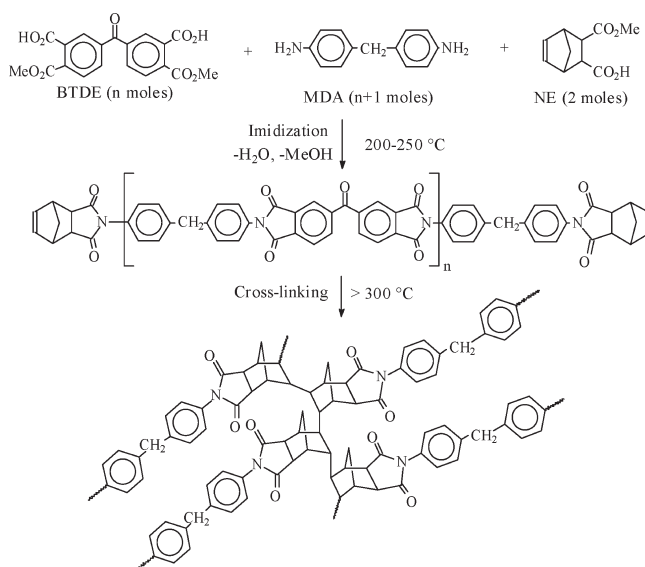


Figure 1. Reaction scheme for the preparation of cross-linked PMR-15 from methylenedianiline (MDA), benzophenonetetracarboxylic diacid diester (BTDE), and nadic acid ester (NE).

*Corresponding author. Fax: 972-3-7384053. E-mail: frimea@mail.biu.ac.il.

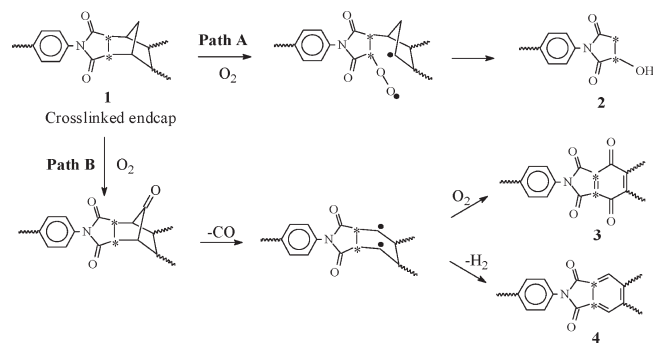


Figure 2. Nadic end-cap degradation pathways (* = ^{13}C labeled carbons).

lead to lower weight loss in addition polyimides, and result in less shrinkage and cracking in the oxidation layer.⁶

We recently reported our studies on 1,2,3,6-tetrahydrophthalic (THP) end-capped bisimides **5** (Figure 3) that contain *no bridging methylene group* at all.⁸ This structure was first investigated by TRW and NASA in the 1980s and found to yield composites with thermal oxidative stability (TOS) values *better* than PMR-15, but which were quite frangible and brittle.^{9,10} No explanation for these peculiar results was given, however. When the thermolysis of variously substituted MDA 1,2,3,6-tetrahydrophthalic bismides **5** up to 371 °C was explored, it became evident that aromatization competes with cross-linking. Indeed, as a result of aromatization, cross-linking was lowered to < 40% of the reaction product. The high aromatic fraction is presumably responsible for the observed improved thermal oxidative stability of THP end-capped polyimides, while the concomitantly lowered amount of cross-linking resolves the source of their substantial frangibility.

The mechanism for aromatization was further shown to be an oxidative one,⁸ since thermolysis of the tetrahydrophthalimides under inert atmosphere dramatically lowers the degree of aromatization. At the same time, the ratio of cross-linking to the degree of aromatization rose from ca. 1:1 in air to almost 10:1 under argon. The residual aromatization observed presumably results from radical induced disproportionation.^{11–16} This finding suggests that highly cross-linked THP polyimides can be prepared but would require special processing conditions such as the use of an inert atmosphere autoclave.

The most labile hydrogens in the THP ring (**5**) are the allylic C-3 and C-6 hydrogens. Hence, 3,3- and/or 6,6-dialkylation should inhibit precuring oxidative aromatization of these THP systems. Alternatively, aromatization could also be attenuated by alkylating the ring juncture carbons C-1 and/or C-2. The present paper describes our attempts in this regard.

Experimental Section

NMR spectra were recorded on a Bruker DRX 200 MHz, Bruker DRX 300 MHz, Bruker DMX 600 MHz or Bruker DMX 700 MHz Fourier transformation spectrophotometer. For 1D NMR spectra QNP probe was used. All 2D experiments (COSY, HMQC, HMBC, and NOSEY) were run and processed by Bruker software. NMR spectra were generally run at 25 ± 1 °C while locked to the deuterium signals of the sample solvent. 1H and ^{13}C NMR chemical shifts are expressed in δ (ppm) relative to TMS (0 ppm) (in $DMSO-d_6$, acetone- d_6 , or $CDCl_3$) as internal standard as reported by Gottlieb.¹⁷

DCI/CH₄ MS and **HRMS** were taken in a AutoSpec Previer high resolution mass spectrometer manufactured by Waters (UK). **FTIR** was collected in a Vector 22 manufactured by Bruker, and the data were processed by Opus 5.0 (Bruker) software. The spectra were analyzed with IR MentorPro 6.5 (Bio-Rad) software. **DSC** was performed using a Mettler TC-15

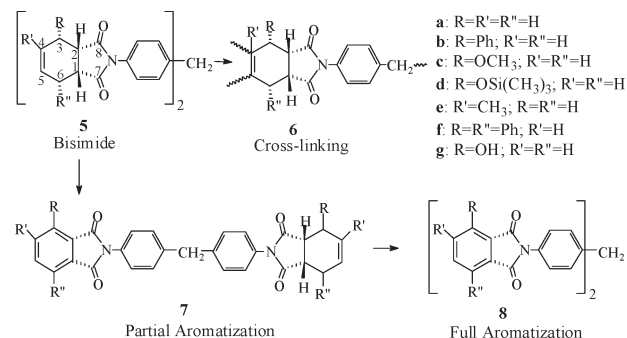


Figure 3. Competition between cross-linking and aromatization in the thermal aging of THP bismides **5**.

system equipped with a DSC-25 calorimetric cell and Mettler STAR eV 7.01 software (Mettler Toledo Inc.). The heating rate employed was 10 °C/min in the temperature range 30–600 °C with 20 mL/min flow of N_2 . To check the reproducibility of results, the calorimetric scan was run twice. **TGA** was performed in a TGA Q500 manufactured by TA Instruments. The data was processed with Universal Analysis 2000, Version 4.2E (TA Instruments) software. The samples were heated from 25 to 950 °C with a heating rate of 10 °C/min and 120 mL/min flow of N_2 . Analytical **TLC** was performed using Merck silica gel microcards. Maleic anhydride (Aldrich), citraconic anhydride (Aldrich), 2,3-dimethylmaleic anhydride (Aldrich), 1,3-butadiene (Aldrich), *trans*-piperylene (Aldrich) methylenedianiline (Aldrich) and 1,2,3,6-tetrahydrophthalic anhydride (Aldrich) were commercially available with purity > 98% and used as supplied. **X-ray crystallography** was carried out on a single crystal of the sample, as described in the Supporting Information.

2,3-Dimethyl-1,6-dihydrophthalic Anhydride (11a) and 2,3-Dimethyl-1,6-dihydrophthalic Dicarboxylic Acid (12a). The procedure below is a modification of that reported by Brocksom and Constantino;¹⁸ the spectral data supplied by these authors is only partial and the full data is given below.

A solution of citraconic anhydride (**10b**) (4.11 g, 0.037 mol) and picric acid (16 μ L) in 20 mL of dry toluene was placed in a corked heavy-wall pressure tube equipped with a magnetic stirrer bar. Ar gas was bubbled through the stirred solution for a few minutes. At this point *trans*-piperylene (**9a**) (5.00 g, 0.0730 mol) was added. The pressure tube was sealed with a Teflon screw stopper, and the reaction mixture was stirred and heated to 110 °C in an oil bath for 7 days, behind a protective shield. The reaction solution was allowed to cool, and all volatiles were rotary evaporated to yield 6.60 g (0.0366 mol, 50% yield) of yellow solid crude, containing a 7:3 mixture of isomers **11a** and **11b**. The crude anhydride mixture was hydrolyzed to diacid without further purification.

The anhydride mixture (**11a** and **11b**) was suspended in a solution of 5.01 g (0.125 mol) of NaOH in 170 mL of H_2O and the reaction mixture was stirred at room temperature overnight. The ice-cooled reaction mixture was acidified (pH paper) by dropwise addition of 14.3 mL of concentrated HCl over 30 min. At this point a white precipitate appeared. The precipitate was dissolved in acetone and filtered (removing NaCl) to yield a 7:3 mixture of **12a** and **12b**. The major product was isolated and purified by recrystallization from H_2O to yield clean white crystals of the diacid **12a** (2.77 g, 0.0144 mol, 39% yield). The remaining mother liquor contains a 1:1 mixture of **12a** and **12b**, which were inseparable.

In a 500 mL round-bottom flask, equipped with a drying tube ($CaCl_2$) and a magnetic stirrer bar, diacid **12a** (2.77 g, 0.0135 mol) was dissolved and stirred at rt in trifluoroacetic anhydride (180 mL) for 4 h. Rotary evaporation of all the volatiles followed by recrystallization of the residue from diethyl ether gives the desired clean anhydride **11a** (1.53 g, 0.0085 mol, 63% yield; overall yield from citraconic acid was 23%).

11a: mp: 48–50 °C. R_f (Et₂O): 0.27. R_f (acetone): 0.28. ¹H NMR (CDCl₃): δ 5.926 (m, 1H, H₅), 5.801 (m, 1H, H₄), 2.993 (dd, J = 7.5, 2.7 Hz, 1H, H₁), 2.749 (ddd, J = 16.5, 5.7, 2.4 Hz, 1H, H₆), 2.275 (m, 1H, H_{6'}), 2.205 (m, 1H, H₃), 1.489 (s, 3H, H₉), 1.226 (d, J = 7.2 Hz, 3H, H₁₀). ¹³C NMR (CDCl₃): δ 174.90 (C₇), 173.36 (C₈), 133.59 (C₄), 126.55 (C₅), 48.93 (C₂), 47.59 (C₁), 37.00 (C₃), 23.28 (C₉), 22.47 (C₆), 16.07 (C₁₀). FTIR (KBr): 3046 (m), 2986 (m), 2942 (m, CH₃), 2881 (m, CH₃), 2862 (m, CH₃), 1846 (s, C=O, C–O–C of anhydride), 1770 (s, C=O, C–O–C of anhydride), 1637 (m, CH=CH), 1380 (m), 1219 (m, C–O–C of anhydride), 1179 (m, C–O), 1029 (m), 960 (s), 952 (s) cm^{−1}. MS (DCI-CH₄) m/z : 181 (MH⁺, 12%), 180 (M⁺, 7%), 153 (MH⁺ – CO, 12%), 152 (M⁺ – CO, 44%), 108 (M⁺ – C₂O₃, 47%), 107 (M⁺ – C₂O₃ – H, 100%), 93 (M⁺ – C₂O₃ – CH₃, 74%), 91 (M⁺ – C₂O₃ – CH₃ – 2H, 31%). HRMS (DCI-CH₄) m/z : calcd for C₁₀H₁₂O₃ (MH⁺), 181.0865; found, 181.0857.

12a: mp: 191 °C. R_f (acetone): 0.08. ¹H NMR (acetone-*d*₆): δ 5.70 (dq, J = 10, 3 Hz, 1H, H₅), 5.37 (dq, J = 10, 2 Hz, 1H, H₄), 2.74 (dddt, J = 17, 11, 4, 2.5 Hz, 1H, H₆), 2.64 (dd, J = 11, 5.5 Hz, 1H, H₁), 2.30 (dt, J = 17, 5.5, 2 Hz, 1H, H_{6'}), 2.22 (qsex, J = 6, 2 Hz, 1H, H₃), 1.31 (s, 3H, H₉), 1.02 (d, J = 6 Hz, 3H, H₁₀). ¹³C NMR (acetone-*d*₆): δ 174.42 (C₇), 173.81 (C₈), 129.92 (C₄), 124.71 (C₅), 48.76 (C₁), 44.70 (C₂), 39.05 (C₃), 27.69 (C₆), 23.42 (C₉), 15.17 (C₁₀). FTIR (KBr): 3034–2857 (vbs, OH, C=C and CH₃), 2608 (b), 1703 (s, C=O), 1473 (w), 1452 (w, COOH), 1428 (w, CH₂), 1276 (w), 1236 (w, C–O), 1203 (w), 1013 (m), 969 (m), 954 (m), 938 (m), 891 (w), 846 (w), 690 (m) cm^{−1}. MS (DCI-CH₄) m/z : 199 (MH⁺, 31%), 182 (MH⁺ – OH, 7%), 181 (MH⁺ – H₂O, 61%), 180 (M⁺ – H₂O, 17%), 153 (M⁺ – COOH, 34%), 152 (M⁺ – H₂O – CO, 40%), 108 (M⁺ – H₂O – C₂O₃, 25%), 107 (M⁺ – H₂O – C₂O₃ – H, 100%), 93 (M⁺ – H₂O – C₂O₃ – CH₃, 29%), 91 (M⁺ – H₂O – C₂O₃ – CH₃ – 2H, 26%). HRMS (DCI-CH₄) m/z : calcd for C₁₀H₁₄O₄ (MH⁺), 199.0970; found, 199.0978.

1,2,3-Trimethyl-6-monohydrophthalic Anhydride (11c). A solution of 2,3-dimethyl maleic anhydride (**10c**) (4.63 g, 0.03672 mol), and picric acid (16 μL) in 50 mL of dry toluene was placed in a corked heavy-wall pressure tube equipped with a magnetic stirrer bar. Argon was bubbled through the stirred solution for a few minutes. At this point *trans*-piperylene (**9a**) (5.00 g, 0.07340 mol) was added to the reaction mixture. The pressure tube was sealed with a Teflon screw stopper, and the reaction mixture was stirred and heated to 120 °C in an oil bath, for 16 weeks, behind a protective shield. All the volatiles were then rotary evaporated to yield a yellow oil containing the desired product (8.5 g, 90% yield). The crude product was purified by recrystallization from hot diethyl ether. Yield: 72% (6.81 g, 0.035 mol).

11c: Mp: 83 °C. R_f (acetone): 0.64. R_f (Et₂O): 0.60. ¹H NMR: (CDCl₃): δ 5.947 (m, 1H, H₅), 5.732 (m, 1H, H₄), 2.671 (dd, J = 15.9, 6.6 Hz, 1H, H₆), 2.161 (m, 1H, H₃), 1.986 (dm, J = 15.9 Hz, 1H, H_{6'}), 1.362 (s, 3H, H₁₀), 1.348 (s, 3H, H₉), 1.300 (d, J = 7.5 Hz, 3H, H₁₁). ¹³C NMR (CDCl₃): δ 176.94 (C₇), 174.69 (C₈), 134.53 (C₄), 127.75 (C₅), 52.05 (C₂), 50.15 (C₁), 37.84 (C₃), 33.02 (C₆), 21.07 (C₉), 18.30 (C₁₀), 15.86 (C₁₁). FTIR (KBr): 3050 (m CH₂), 2994 (m, CH₂), 2979 (m, CH₂), 2945 (m, CH₃), 2885 (m, CH₃), 2854 (w, CH₂), 1842 (m, C=O, anhydride), 1767 (s, C=O, anhydride), 1223 (m, C–O–C of anhydride), 992 (s) cm^{−1}. MS (DCI-CH₄) m/z : 195 (MH⁺, 1%), 180 (MH⁺ – CH₃, 4%), 166 (M⁺ – CO, 16%), 122 (M⁺ – C₂O₃, 37%), 121 (MH⁺ – CO₂ – 2CH₃, 20%), 108 (MH⁺ – C₂O₃ – CH₃, 9%), 107 (M⁺ – C₂O₃ – CH₃, 100%), 91 (M⁺ – C₂O₃ – CH₃ – CH₄, 30%). HRMS (DCI-CH₄) m/z : calcd for C₁₁H₁₄O₃ (MH⁺), 195.1021; found, 195.1002.

5,2,2,4 3,3-Dimethyl-1,2,6-trihydrophthalic Anhydride (11d). The procedure below is based on that described by Gosselin et al. for the preparation of the 3,3,4-trimethyl analogue.¹⁹ The ¹³C NMR data corresponds to the partial data supplied for **11d** by Alemany and Brown²⁰ and for the 3,3,4-trimethyl analogue by Gosselin.¹⁹ Our ¹H NMR and IR data do not correspond at all to that given by Stokes and Welker²¹ for **11d**. Indeed, the latter report only a single carbonyl absorption in the IR, when

our double absorptions at 1848 and 1777 is what is expected for an anhydride. The latter might well correspond to the hydrolyzed diacid analogue; compare the data of **11a** vs **12a**.

Maleic anhydride (**10a**) (8.57 g, 0.087 mol, 4 equiv) and hydroquinone (0.24 g, 0.0022 mol, 0.1 equiv) were dissolved in 25 mL of dry THF in a 100 mL heavy-wall pressure tube equipped with a magnetic stirrer bar. Ar was bubbled through the stirred solution for a few minutes and 4-methyl-1,3-pentadiene (**9b**) (1.795 g, 2.5 mL, 0.022 mol, 1 equiv) was added to the reaction mixture. The pressure tube was sealed with a Teflon screw stopper, and the reaction mixture was heated to 100 °C (oil bath), and stirred for 24 h, behind a protective shield. All the volatiles were removed under reduced pressure, and the unreacted maleic anhydride was distilled out (50–55 °C/0.05 mmHg). The residual yellow oil was dissolved in 10 mL of CHCl₃, gravity-filtered and rinsed with more 10 mL of CHCl₃ to remove the insoluble hydroquinone. The solvent was removed under reduced pressure and the crude was purified by distillation at 65–70 °C/0.05 mmHg (2.38 g, 0.0132 mol, 60% yield).

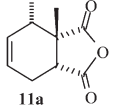
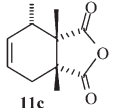
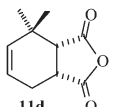
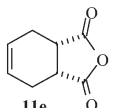
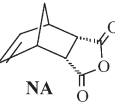
11d. Mp: 66–68 °C. R_f (Et₂O): 0.62. R_f (acetone): 0.51. ¹H NMR (CDCl₃): δ 5.734 (m, 1H, H₅), 5.727 (m, 1H, H₄), 3.43 (dt, J = 10, 7.5 Hz, 1H, H₁), 2.945 (d, J = 10 Hz, 1H, H₂), 2.555 (m, 2H, H₆), 1.316 (s, 3H, H₉), 1.008 (s, 3H, H₁₀). ¹³C NMR (CDCl₃): δ 174.47 (C₇), 171.59 (C₈), 137.41 (C₄), 123.40 (C₅), 50.00 (C₂), 38.36 (C₁), 33.31 (C₃), 28.68 (C₆), 23.93 (C₁₀), 20.34 (C₉). FTIR (KBr): 3602 (m, CH=CH), 3030 (m, C=C), 2964 (m, CH₃), 2932 (m, CH₂), 2899 (m, CH₂), 2875 (m, CH₃), 2877 (m, C–O–C, CH₃), 1848 (s, C=O), 1777 (s, C=O), 1727 (m, C=O), 1624 (m, C=O), 1464 (w, CH₂), 1369 (m, CH₃), 1328, 1295, 1195 (m), 1087 (m, C–O anhydride), 1006 (m, C=O anhydride), 919 (w), 896 (w), cm^{−1}. MS (DCI-CH₄) m/z : 181 (MH⁺, 55%), 180 (M⁺, 17%), 153 (MH⁺ – CO, 24%), 152 (M⁺ – CO, 68%), 107 (M⁺ – C₂O₃ – H, 100%), 93 (M⁺ – C₂O₃ – CH₃, 85%), 91 (M⁺ – H₂O – C₂O₃ – CH₃ – 2H, 43%). HRMS (DCI-CH₄) m/z : calcd for C₁₀H₁₂O₃ (MH⁺), 181.0865; found, 181.0900.

Preparation of Monoimides 13a, 13c, 13d, and 13e. End-cap (anhydrides **11a**, **11c**, **11d**, or **11e**) and MDA in an equimolar ratio were ground together and placed in an open dark glass bottle. The mixture was heated in a oven for 1 h at 204 °C (400 °F). The reaction product was cooled, weighed, ground to a powder, and a sample was removed for spectroscopic analysis. On the basis of the C₁₃ dibenzyl methylene, the major product was monoimide **13** (ca. 50%), accompanied by smaller amounts of bisimide **16** (ca. 20%), MDA (ca. 30%) and amic acids **14** and **15** (negligible amounts).

13a. ¹H NMR (CDCl₃): δ 7.231 (AA'/BB'm, 2H, H₁₁), 7.124 (AA'/BB'm, 2H, H₁₀), 6.804 (AA'/XX'm, 2H, H_{11'}), 6.611 (AA'/XX'm, 2H, H_{10'}), 5.921 (m, 1H, H₅), 5.799 (m, 1H, H₄), 3.877 (s, 2H, H₁₃), 3.300 (bs, 2H, NH₂), 2.821 (dd, J = 7.5, 3.9 Hz, 1H, H₁), 2.794 (ddd, J = 16.5, 5.7, 2.4 Hz, 1H, H₆), 2.300 (dm, J = 16.5, 1H, H_{6'}), 2.248 (m, 1H, H₃), 1.477 (s, 3H, H₁₅), 1.256 (d, J = 7.2 Hz, 3H, H₁₄). ¹³C NMR (CDCl₃): δ 180.15 (C₇), 178.34 (C₈), 144.63 (C₉), 142.36 (C₉), 134.44 (C₄), 130.47 (C_{12'}), 129.87 (C₁₂), 129.62 (C_{11'}), 129.40 (C₁₁), 126.47 (C₅), 126.31 (C₁₀), 115.30 (C_{10'}), 48.09 (C₁), 47.11 (C₂), 40.71 (C₁₃), 37.82 (C₃), 23.56 (C₁₅), 23.32 (C₆), 15.66 (C₁₄). MS (DCI-CH₄) m/z : 361 (MH⁺, 100%), 360 (M⁺, 94%), 268 (M⁺ – C₆H₆N, 27%), 106 (C₇H₅N⁺, 60%). HRMS (DCI-CH₄) m/z : calcd for C₂₃H₂₅N₂O₂ (MH⁺), 361.1916; found, 361.1902.

13c. ¹H NMR (CDCl₃): δ 7.207 (AA'/BB'm, 2H, H₁₁), 7.089 (AA'/BB'm, 2H, H₁₀), 6.942 (AA'/BB'm, 2H, H_{11'}), 6.595 (AA5BB'm, 2H, H_{10'}), 5.939 (m, 1H, H₅), 5.719 (m, 1H, H₄), 3.863 (s, 2H, H₁₃), 3.380 (bs, 2H, NH₂), 2.702 (dd J = 15.6, 7.2 Hz, 1H, H₆), 2.175 (m, 1H, H₃), 1.968 (dm J = 15 Hz, 1H, H_{6'}), 1.359 (s, 3H, H₁₅), 1.326 (d, J = 7.2 Hz, 3H, H₁₄), 1.325 (s, 3H, H₁₆). ¹³C NMR (CDCl₃): δ 181.73 (C₈), 179.89 (C₇), 144.63 (C₉), 142.26 (C₉), 135.31 (C₄), 130.45 (C_{12'}), 129.82 (C₁₂), 129.59 (C_{11'}), 129.34 (C₁₁), 128.19 (C₅), 126.33 (C₁₀), 115.27 (C_{10'}), 50.63 (C₂), 49.23 (C₁), 40.69 (C₁₃), 38.55 (C₃), 33.69 (C₆), 21.14 (C₁₆), 18.20 (C₁₅), 15.69 (C₁₄). MS (DCI-CH₄) m/z : 375 (MH⁺,

Table 1. Product Distribution (%)^a of End-Caps 11a–e and Nadic Anhydride (NA) Reacted with MDA in a 2:1 Ratio (13, Monoimide; 14, Bisamic Acid; 15, Monoimide Monoamic Acid; 16, Bisimide; 17, Bisphthalimide; 18, Cross-Linked Bisimide; 19, Cross-Linked Phthalimides)

Anhydride (11)	Product	H ₁₃ (ppm)	204 °C (1 h)	315 °C (30 min)	343 °C (50 min)	371 °C (30 min)
	13a	3.877	0.0	0.0	0.0	0.0
	14a+15a	3.957, 3.927	29.9	7.9	5.6	5.1
	16a	4.007	70.1	89.5	84.8	59.5
	18a	4.017	0.0	2.6	7.6	27.0
	17 and 19	4.051	0.0	0.0	2.0	8.4
	13c	3.869	0.0	0.0	0.0	0.0
	14c+15c	3.963, 3.951, 3.928, 3.915	57.5	33.3	24.1	22.9
	cis,trans-16c	3.996	42.5	62.5	48.2	10.5
	18c	4.025	0.0	4.2	4.8	31.2
	17 and 19	4.051	0.0	0.0	0.0	1.8
	23	4.006	0.0	0.0	22.9	33.6
	13d	3.888	0.0	0.0	0.0	0.0
	14d+15d	3.981, 3.969, 3.939, 3.917	33.3	17.9	10.1	9.8
	cis-16d	4.029	63.6	66.1	8.8	5.61
	trans-16d'	4.029 ^b	3.1	16.0	2.2	1.5
	18d	4.035	0.0	0.0	68.6	58.5
	17 and 19	4.064	0.0	0.0	10.4	24.6 ^c
	13e	3.878	0.0	0.0	0.0	0.0
	14e+15e	3.962, 3.949	16.5	3.5	0.0	0.0
	16e	4.014	83.5	89.5	90.7	64.5
	18e	4.023	0.0	7.0	8.5	26.9
	17 and 19	4.051	0.0	0.0	0.8	8.6
	Monoimide	3.864	5.0	0.0	0.0	0.0
	Imide amic acid	3.880	16.0	0.0	0.0	0.0
	Bisimide	3.976, 4.002 ^d	79.0	73.0	0.0	0.0
	Cross-linked Bisimide	4.026	0.0	27.0	100.0	100.0

^a Product yields were based on the relative integration of C-13 methylene. ^b The methylene hydrogens of both the *cis*- and *trans*-16d presumably resonate at the chemical shift. The relative yields of the two isomers were based on the relative integration of the C-3 methyls. ^c See discussion; this value contains ca. 10% of aromatized cross-linked product 19. ^d Two different peaks were observed corresponding to the *endo* and *exo* isomers.

41%), 374 (M⁺, 42%), 282 (M⁺ – C₆H₆N, 12%), 106 (C₇H₈N⁺, 100%). HRMS (DCI-CH₄) *m/z*: calcd for C₂₄H₂₆N₂O₂ (M⁺), 374.1994; found, 374.2008; calcd for C₂₄H₂₇N₂O₂ (MH⁺), 375.2073; found, 375.2072.

13d. ¹H NMR (CDCl₃): δ 7.258 (AA'BB'm, 2H, C₁₁), 7.177 (AA'BB'm, 2H, C₁₀), 6.957 (AA'XX'm, 2H, H_{11'}), 6.612 (AA'XX'm, 2H, H_{10'}), 5.782 (m, 1H, H₅ and H₄), 3.886 (s, 2H, H₁₃), 3.350 (bs, 2H, NH₂), 3.265 (m, 1H, H₁), 2.823 (d, *J* = 9.6 Hz, 1H, H₂), 2.575 (m, 2H, H₆), 1.375 (s 3H, H₁₄), 1.013 (s 3H, H₁₅). ¹³C NMR (CDCl₃): δ 179.41 (C₇), 177.37 (C₈), 144.64 (C₉), 142.45 (C₉), 138.48 (C₄), 130.44 (C_{12'}), 129.89 (C₁₂), 129.62 (C₁₁), 129.48 (C_{11'}), 126.27 (C₁₀), 124.05 (C₅), 115.37 (C_{10'}), 49.59 (C₂), 40.72 (C₁₃), 38.64 (C₁), 34.34 (C₃), 29.36 (C₁₄), 23.22 (C₁₅), 21.10 (C₆). MS (DCI-CH₄) *m/z*: 361 (MH⁺, 87%), 360 (M⁺, 100%), 268 (M⁺ – C₆H₆N, 44%), 106 (C₇H₈N⁺, 55%). HRMS (DCI-CH₄) *m/z*: calcd for C₂₃H₂₄N₂O₂ (M⁺), 360.1838; found, 360.1806; calcd for C₂₃H₂₅N₂O₂ (MH⁺), 361.1916; found, 361.1886.

13e. ¹H NMR (CDCl₃): δ 7.233 (AA'BB'm, 2H, C₁₁), 7.136 (AA'BB'm, 2H, C₁₀), 6.955 (AA'XX'm, 2H, H_{11'}), 6.611 (AA'XX'm, 2H, H_{10'}), 5.969 (m, 2H, H₄ and H₅), 3.878 (s, 2H, H₁₃), 3.270 (bs, 2H, NH₂), 3.237 (dm, *J* = 3 Hz, 2H, H₁ and H₂), 2.706 (dm, *J* = 13.2 Hz, 2H, H₃ and H₆), 2.301 (dm, *J* = 13.2 Hz, 2H, H_{3'} and H_{6'}). ¹³C NMR (CDCl₃): δ 179.24 (C₇ and C₈), 144.64 (C₉), 142.52 (C₉), 130.41 (C_{12'}), 130.25 (C₁₂), 129.69 (C₁₁), 129.45 (C_{11'}), 127.84 (C₄ and C₅), 126.47 (C₁₀), 115.33 (C_{10'}), 40.71 (C₁₃), 39.24 (C₁ and C₂), 23.78 (C₃ and C₆). MS (DCI-CH₄) *m/z*: 333 (MH⁺, 26%), 332 (M⁺, 13%), 240 (M⁺ – C₆H₆N, 15%), 227 (MH⁺ – C₇H₈N, 7%), 199 (MH⁺ – C₈H₆O₂, 59%), 198 (MH⁺ – C₈H₇O₂, 36%), 197 (MH⁺ – C₈H₈O₂, 12%), 106 (C₇H₈N⁺, 100%). HRMS (DCI-CH₄) *m/z*: calcd for C₂₁H₂₀N₂O₂ (M⁺), 332.1525; found, 332.1531; calcd for C₂₂H₂₀N₂O₂ (MH⁺), 333.1603; found, 333.1588.

Thermolysis of a 2:1 Mixture of Anhydrides 11 and MDA. A 2:1 mixture of end-cap (anhydrides 11a, 11c, 11d or 11e), and MDA were ground together and placed in an open dark glass bottle. The mixture was heated in Carbolite ELF 11/6B oven for 1 h at 204 °C (400 °F), then at 315 °C (600 °F) for 30 min, at 340 °C (650 °F) for 50 min, and finally at 371 °C (700 °F) for 30 min. After each step, the reaction product was cooled, weighed, and ground to a powder, and a sample was removed for spectroscopic analysis (liquid and solid state ¹H and ¹³C NMR, MS/HRMS, DSC, FTIR, and TGA). With the exception of 11c, bisimide 16 was the predominant product after heating to 204 °C; at 315 °C, bisimide 16 predominated for all the systems studied, and its spectral data could be easily extracted from the reaction mixture at either point. In the case of 11c and 11d, bisimide isomers 16c' and 16d' were also observed (see text and Table 1).

Aromatization of 11e yields 17e, whose spectral data has been previously reported.⁸ Full aromatization of compounds 11a, 11c and 11d yields *o*-methylphthalimide 17a, whose partial NMR data could be extracted from the reaction mixture. The C-3 methyl of 17a appears at 2.74 ppm, which corresponds to the chemical shift of this methyl in 3-methylphthalic anhydride (2.74 ppm)²² and *N*-(pyridine-2-ylmethyl)-3-methylphthalimide (2.71 ppm).²³ In addition, it has a very distinctive doublet at 7.5 (H₄), triplet at 7.6 (H₅) and doublet at 7.8 (H₆) ppm. Some of the other NMR data is unavailable because it overlaps with the larger peaks of other molecules. A singlet presumably corresponding to H₆ of 19a is observed at 7.262 ppm.

In the thermolysis of a 2:1 mixture of anhydride 11c and MDA, retro Diels–Alders product bis-dimethylmaleimide (23) was observed at 343 °C (22.9% of the mixture) and at 371 °C (33.6%). It was characterized based on its partial NMR data,

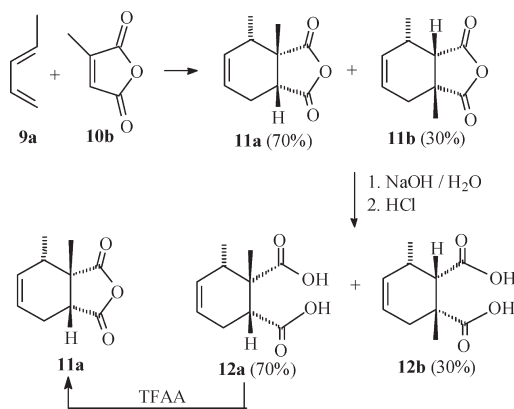


Figure 4. Preparation of 2,3-dimethyl-*cis*-1,6-dihydrophthalic anhydride (**11a**).

which corresponds very well to that reported²⁴ for *N*-phenyl-2,3-dimethylmaleimide.

16a. ¹H NMR (CDCl₃): δ 7.240 (AA'/BB'm, 4H, H₁₁), 7.149 (AA'/BB'm, 4H, H₁₀), 5.926 (m, 2H, H₅), 5.810 (m, 2H, H₄), 4.007 (s, 2H, H₁₃), 2.833 (dd *J* = 7.5, 2.7 Hz, 2H, H₁), 2.798 (ddd *J* = 16.2, 5.7, 2.7 Hz, 2H, H₆), 2.356–2.204 (m, 4H, H₃ and H_{6'}), 1.484 (s, 6H, H₁₅), 1.256 (d, *J* = 7.2 Hz, 6H, H₁₄). ¹³C NMR (CDCl₃): δ 180.08 (C₇), 178.29 (C₈), 140.76 (C₉), 134.42 (C₄), 130.24 (C₁₂), 129.63 (C₁₁), 126.87 (C₅), 126.50 (C₁₀), 48.07 (C₁), 47.42 (C₂), 41.12 (C₁₃), 37.82 (C₃), 23.54 (C₁₅), 23.31 (C₆), 15.66 (C₁₄). FTIR (KBr): 1778 (m, C=O imide), 1704 (vs, C=O imide), 1635 (m, C=C), 1541 (s, C–N imide), 1511 (s, Ar) cm^{−1}.

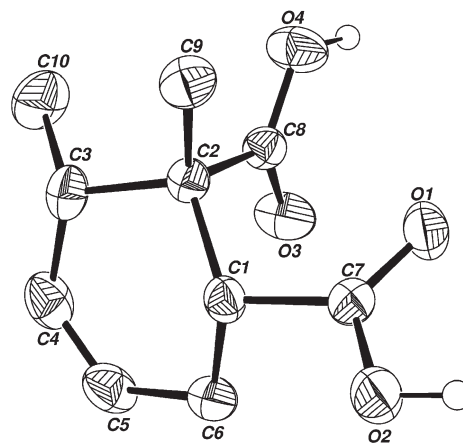
16c. ¹H NMR (CDCl₃): δ 7.209 (AA'/BB'm, 4H, H₁₁), 7.114 (AA'/BB'm, 4H, H₁₀), 5.944 (m, 2H, H₅), 5.726 (m, 2H, H₄), 3.996 (s, 2H, H₁₃), 2.712 (dd *J* = 15, 7.2 Hz, 2H, H₆), 2.181 (m, 2H, H₃), 1.976 (dm *J* = 15 Hz, 2H, H_{6'}), 1.370 (s, 6H, H₁₅), 1.332 (d, *J* = 7.2 Hz, 6H, H₁₄), 1.333 (s, 6H, H₁₆). ¹³C NMR (CDCl₃): δ 181.68 (C₈), 179.83 (C₇), 140.70 (C₉), 135.32 (C₄), 129.93 (C₁₂), 129.56 (C₁₁), 128.21 (C₅), 126.49 (C₁₀), 50.67 (C₂), 49.25 (C₁), 41.11 (C₁₃), 38.58 (C₃), 33.71 (C₆), 21.16 (C₁₆), 18.22 (C₁₅), 15.70 (C₁₄). FTIR (KBr): 1774 (m, C=O imide), 1702 (vs, C=O imide), 1512 (s, Ar) cm^{−1}.

cis-16d. ¹H NMR (CDCl₃): δ 7.261 (AA'/BB'm, 4H, H₁₁), 7.210 (AA'/BB'm, 4H, H₁₀), 5.760 (m, 4H, C₄ and H₅), 4.029 (s, 2H, H₁₃), 3.279 (dt, *J* = 9.6, 7.5 Hz, 2H, H₁), 2.835 (d, *J* = 9.6 Hz, 2H, H₂), 2.575 (m, 4H, H₆), 1.380 (s, 3H, H₁₄), 1.018 (s, 3H, H₁₅). ¹³C NMR (CDCl₃): δ 179.38 (C₇), 177.34 (C₈), 140.83 (C₉), 138.45 (C₄), 130.14 (C₁₂), 129.74 (C₁₁), 126.45 (C₁₀), 124.05 (C₅), 49.58 (C₂), 41.14 (C₁₃), 38.63 (C₁), 34.35 (C₃), 29.34 (C₁₄), 23.20 (C₁₅), 21.08 (C₆). FTIR (KBr): 1775 (m, C=O imide), 1702 (vs, C=O imide), 1635 (m, C=C), 1512 (s, Ar) cm^{−1}.

trans-16d'. ¹H NMR (CDCl₃): δ 7.280 (AA'/BB'm, 4H, H₁₁), 7.210 (AA'/BB'm, 4H, H₁₀), 5.660 (ddd, *J* = 10, 5.5, 2 Hz, 2H, H₅), 5.495 (ddd, *J* = 10, 2.5, 1.5 Hz, 2H, C₄), 4.029 (s, 2H, H₁₃), 2.620 (d, *J* = 11.5 Hz, 2H, H₂), 2.929 (td, *J* = 11.5, 5 Hz, 2H, H₁), 2.590 (dddd, *J* = 17.5, 5.5, 5, 1.5 Hz, 2H, H₆), 2.322 (dddd, *J* = 17.5, 11.5, 2.5, 2 Hz, 2H, H_{6'}), 1.392 (s, 6H, H₁₄), 1.176 (s, 6H, H₁₅). ¹³C NMR (CDCl₃): δ 176.07 (C₈), 174.76 (C₇), 140.88 (C₁₂), 139.80 (C₄), 130.58 (C₉), 129.67 (C₁₁), 126.34 (C₁₀), 123.02 (C₅), 52.77 (C₂), 41.13 (C₁₃), 39.90 (C₁), 33.13 (C₃), 28.49 (C₁₄), 25.59 (C₆), 22.44 (C₁₅).

16e. ¹H NMR (CDCl₃): δ 7.247 (AA'/BB'm, 4H, C₁₁), 7.159 (AA'/BB'm, 4H, C₁₀), 5.973 (m, 4H, H₄ and H₅), 4.014 (s, 2H, H₁₃), 3.247 (m, 4H, H₁ and H₂), 2.706 (dm, *J* = 14 Hz, 4H, H₃ and H₆), 2.306 (dm, *J* = 14 Hz, 4H, H_{3'} and H_{6'}). ¹³C NMR (CDCl₃): δ 179.38 (C₇ and C₈), 140.99 (C₉), 130.39 (C₁₂), 129.81 (C₁₁), 127.96 (C₄ and C₅), 126.60 (C₁₀), 41.26 (C₁₃), 39.37 (C₁ and C₂), 23.90 (C₃ and C₆). FTIR (KBr): 1774 (m, C=O imide), 1703 (C=O imide), 1625 (m, C=C), 1512 (Ar) cm^{−1}.

17a. ¹H NMR (CDCl₃): δ 7.778 (d, *J* = 7.5 Hz, 1H, H₆), 7.631 (t, *J* = 7.5 Hz, 1H, H₅), 7.524 (d, *J* = 7.5 Hz, 1H, H₄), 4.051 (s, 2H, H₁₃), 2.74 (s, 3H, CH₃ at C-3) ppm.



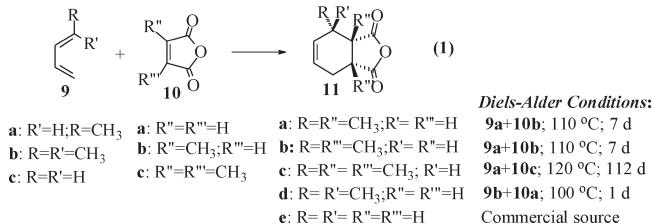
12a

Figure 5. X-ray structure of 2,3-dimethyl-1,6-dihydrophthalic dicarboxylic acid (**12a**).

23. ¹H NMR (CDCl₃): δ 4.005 (s, 2H, CH₂), 2.050 (s, 6H, CH₃). ¹³C NMR (CDCl₃): δ 170.98 (C=O), 137.41 (C=C), 8.92 (CH₃). [Lit.²⁴ *N*-phenyl-2,3-dimethylmaleimide: 170.4 (C=O); 137.4 (C=C); 8.8 (CH₃)].

Results and Discussion

Preparation of THP End-Caps. Alkylated tetrahydrophthalic (THP) anhydrides **11a–d** were synthesized for possible use as end-caps via the Diels–Alder cycloaddition²⁵ of the corresponding butadienes **9** and maleic anhydrides **10** (eq 1), according to modified literature procedures.^{18,19}



The cycloaddition of *trans*-piperylene (**9a**) to citraconic anhydride (**10b**) yields a mixture of isomers **11a** and **11b** in 7:3 ratio.¹⁸ In order to isolate the products, the anhydrides mixture was hydrolyzed under basic conditions yielding diacids **12a** and **12b** (in the same 7:3 ratio). Recrystallization of the mixture yields pure diacid **12a**, with a 1:1 mixture of **12a** and **12b** in the mother liquor. Diacid **12a** was cyclized to the corresponding anhydride **11a** (in an overall yield of 40%) with trifluoroacetic anhydride (see Figure 4).

X-ray analysis²⁶ of diacid **12a** confirms that the methyls on C-2 and C-3 lie *trans* to each other and the anhydride/diacid are *trans* to C-10, as shown in Figure 5.

The preference for the formation of **11a** (“ortho” product; see Figure 6) over **11b** (“meta” product) is well-known²⁷ and consistent with Houk’s rule^{28,29} regarding the matching of frontier molecular orbital (FMO) coefficients, in which “large prefers large” and “small prefers small”.

Because of symmetry considerations, in the cycloaddition reaction between *trans*-piperylene (**9a**) and 2,3-dimethylmaleic anhydride (**10c**), as well as between 4-methyl-1,3-pentadiene (**9b**) and maleic anhydride (**10a**), only one possible product can result in each case—namely, anhydrides **11c** and **11d** respectively. 2D-NMR experiments as well as X-ray analysis confirm the structure of the products as shown in eq 1. In particular, the anhydride ring of **11c** is *cis* to the C-3

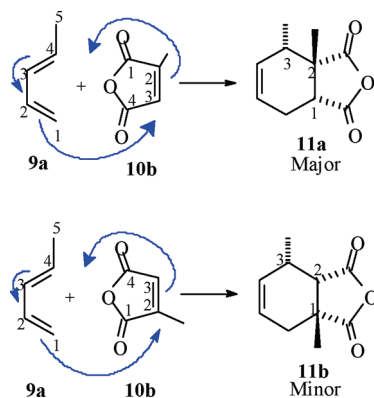


Figure 6. Relative orientation of the Diels-Alder cycloaddition of *trans*-piperylene (**9a**) with citraconic anhydride (**10b**).

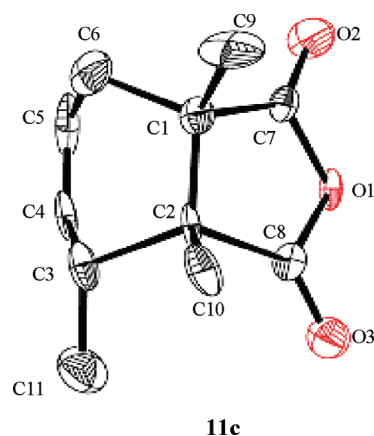


Figure 7. X-ray structure of 1,2,3-trimethyl-6-monohydrophthalic anhydride (**11c**).

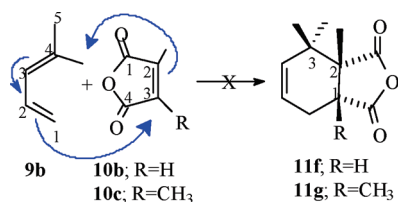


Figure 8. Expected cycloaddition of 4-methyl-1,3-pentadiene (**9b**) with citraconic anhydride (**10b**) or 2,3-dimethylmaleic anhydride (**10c**).

methyl, where the C-1-, C-2- and C-3-methyls lie *cis,trans* to each other (see Figure 7).²⁵ The X-ray analysis also reveals that the length of the double bond between C-5 and C-6 in **11c** is 1.3240 Å.

Unfortunately, 4-methyl-1,3-pentadiene (**9b**) resisted any reaction between mono and dimethylmaleic anhydrides **9b** and **9c** (Figure 8). Even when the cycloadditions was carried out in a sealed tube at 140 °C for 6 months, NMR analysis showed only unreacted starting materials. Presumably, the cycloaddition is inhibited by steric interference of the *Z*-methyl group on C-4 of **9b**. The latter prevents 2-methylated anhydrides **10b** and **10c** from approaching beneath the diene, precluding the requisite secondary overlap interactions between the LUMO of the dienophile and the HOMO of the diene in the transition state.^{30,31}

Thermolysis of THP Bisimides 16. With the THP end-caps now in hand, their thermal reaction with MDA was explored. Anhydrides **11a**, **11c**, and **11d**, and the commercially available *cis*-1,2,3,6-tetrahydrophthalic anhydride (**11e**), were

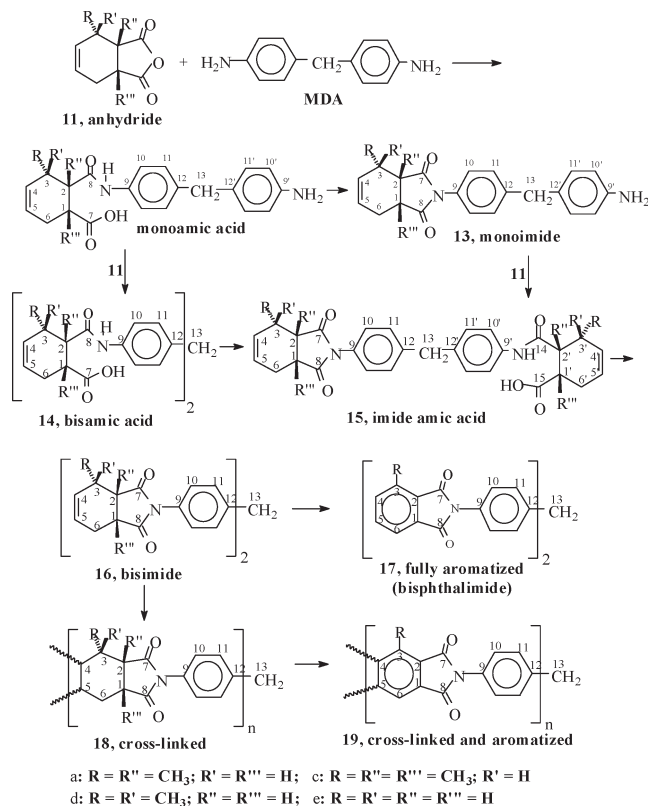


Figure 9. Reaction of substituted tetrahydrophthalic anhydride end-caps **11** with MDA.

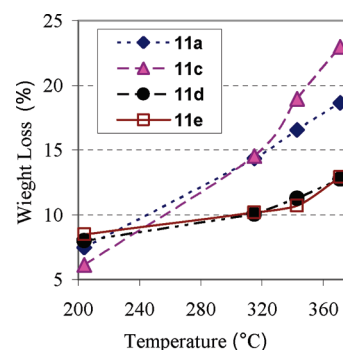


Figure 10. Weight loss on cure and thermolysis of bisimides **16** formed from 1:2 mixtures of MDA and anhydrides **11**. Imidization only accounts for ca. 5% of the weight loss observed.

ground together with MDA in a 2:1 ratio and carried through 4 thermal steps: (1) 204 °C (400 °F, 60 min); (2) 315 °C (600 °F, 30 min); (3) 343 °C (650 °F, 50 min); and (4) 371 °C (700 °F, 30 min). After each heating step, a sample was removed for analysis. The various products were identified by proton and carbon NMR (*vide infra*), based on our previous experience with related systems.⁸ Figure 9 summarizes the major transformations believed to be occurring in these reactions, while Table 1 and Figure 10 track the distribution of products **13–19** and the weight loss, respectively, as one proceeds along the thermal steps.³² For comparison Table 1 includes the results obtained with nadic anhydride (NA).

Before analyzing the results, it is necessary to explain how the product distribution was determined. As mentioned previously, the chemical shift of the H-13 hydrogens on the central C-13 methylene group of MDA is amazingly sensitive to the nature of the substituents attached to the amines on

Table 2. Product Distribution^a in the Reaction of Anhydrides **11a–e** with MDA in 1:1 Ratio for 1 h at 204 °C.^b

anhydride 11	monoimide 13	bisimide 16	MDA
a	46.3	17.6	36.1
c	52.0	15.9	32.1
d	53.6	20.0	26.4
e	45.5	32.6	21.9

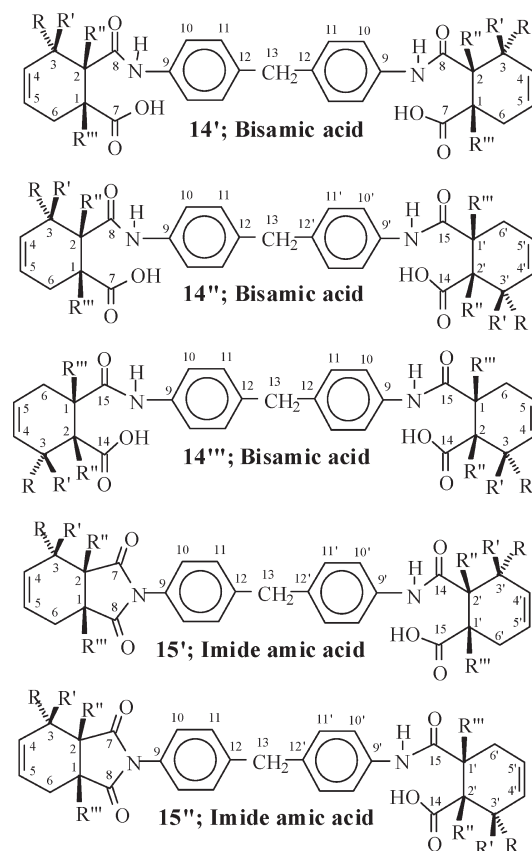
^a Product distribution based on C₁₃ methylene of MDA. ^b Mono- and bisamic acids (upfield of imides) were also observed, but their yield was very small and variable and, hence, not included in the calculation.

either side of the MDA moiety.^{8,33,34} In the 600 and 700 MHz, NMR spectrometers we used for analysis, the various C-13 methylene groups were sharp and clearly defined. In the few cases where some overlap was observed, enhancement programs were used to resolve the issue. Thus, for example, the C₁₃-methylene resonates at 3.878 ppm for the unsubstituted THP monimide **13e**, at 4.014 ppm for bisimide **16e**, and at 4.023 ppm for the cross-linked bisimide **18e**. Integration of the various peaks at ca. 4 ppm was used to calculate the product distribution which appears in Tables 1 and 2. These calculations were confirmed by using other distinctive resonances (aliphatic, olefinic, phthalic, etc.). The cross-linking can be readily detected by a decrease in the olefinic absorptions with the concomitant appearance of aliphatic multiplets in the region of 1.5–2.5 ppm. On the other hand, aromatization to *o*-methylphthalimide **17a** in the case of **11a** and **11c** requires the loss of the methyl groups substituted at the ring junctures C-1 and/or C-2; in the case of **11d** to **17a**, one of the two methyls at C-3 must be cleaved; full aromatization of **11e** yields phthalimide **17e**. The spectral data of **17e** has been previously reported.⁸ It has a very distinctive pair of AA'/BB' multiplets located downfield in the region 7.6–8.0 ppm and separated by ca. 0.2 ppm. Monomethylated analogue **17a** has a very distinctive doublet at 7.5 (H₄), triplet at 7.6 (H₅) and doublet at 7.8 (H₆). The C-3 methyl of **17a** (resulting from bisimides **16a**, **16c** and **16d**) appears at 2.74 ppm. This corresponds well to the chemical shift of this methyl in 3-methylphthalic anhydride (2.74 ppm)²² and *N*-(pyridine-2-ylmethyl)-3-methylphthalimide (2.71 ppm).²³ [Typical ¹H NMR spectra of the product mixture from the thermolysis of **16d** appear in the Supporting Information.]

One caveat should be emphasized, however. The aromatic resonances just mentioned may also result from aromatized product **19**, formed at elevated temperatures from the already cross-linked structures **18**. These resonances should appear under the broad aromatic multiplet appearing between 7.4 and 7.2 ppm. As noted in the Introduction, this is actually the desired scenario, where cross-linking occurs through the double bond of the end-cap, followed by the preferred “path B” (Figure 2) degradation on further aging. Unfortunately, it is difficult to distinguish in the peaks at ca. 4 ppm between cross-linked aromatic structures **19** and noncross-linked aromatic structures **17** (see Figure 9). One would expect this aromatization of cross-linked structures to occur only in the highest thermal step. Evidence will be adduced for this process toward the end of this paper.

With these analytic tools, we began to study the spectra of samples resulting from the thermolysis of two equivalents of MDA with the variously substituted THP end-caps:

(I). *First Thermal Step.* The NMR analysis indicates that in the first thermal step (heating to 204 °C for 1 h), MDA condenses at *both* ends with the anhydride yielding bisamic acid **14**, monoimide monoamic acid **15** and bisimide **16**. The formation of these products undoubtedly proceeds via monoimide **13** or its monoamic acid precursor. Indeed, when anhydrides **11a–e** were mixed with MDA in a 1:1 ratio and

**Figure 11.** Isomeric Bisamic Acids **14** and Imide Amic Acids **15**, Precursors to Bisimide **16**.

heated for 1 h at 204 °C, monoimide **13** and bisimide **16** in an approximate ratio of 70:30 were formed accompanied by small amounts of mono- and bisamic acids (see Table 2).

Focusing now on the monoimide monoamic acid **15** and bisamic acids **14**, the C-13 methylene of the amic acids resonate at ca. 3.95 ppm, at a chemical shift in between that of the mono (**13**) and bisimide (**16**) resonances. A multiplicity of the C-13 methylene absorptions in the range of 3.915–3.981 are observed. In light of the unsymmetrical structure of anhydrides **11a–d**, it is not surprising that absorptions in this region are observed which correspond to the various isomeric bisamic (**14'**, **14''**, and **14'''** in Figure 11) and monoimide monoamic acids (**15'** and **15''**) that can be formed on the way to bisimide **16**. Even in the symmetrical **11e** system, two peaks are observed corresponding to H-13 absorptions of **14e** (3.949 ppm, observed at 204 °C only) and **15e** (3.962 ppm, still detectable at 315 °C). In the other unsymmetrical systems not all five possibilities are observed and several can overlap. As the temperature rises, the various amic acid absorptions gradually disappear (*vide infra*) with one or two persisting even up to 371 °C. In the latter case, the chemical shift changes slightly by several hundredths of a ppm; no firm insight as to their identity is readily obvious.

The ratio of bisimide **16** to amic acids (**14** + **15**) is directly related to the amount of ring substitution. Thus, in the unsubstituted THP system **11e**, this ratio is 5:1; for the disubstituted **11a** and **11d** systems this ratio drops dramatically to ca. 2:1; while for the trisubstituted **11c** it is approximately 2:3. It is likely that as ring substitution increases, so does the steric inhibition to reaction of the anhydride with MDA. This is because ring-opening converts the planar anhydride ring to a congested amic acid moiety. In addition, subsequent imidization via nucleophilic attack of the now

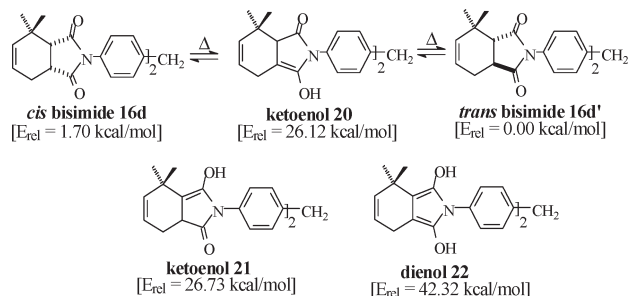


Figure 12. Proposed mechanism for the *cis*-*trans* isomerization of bisimide **16d** to **16d'** and the calculated relative energy (E_{rel}) of various related tautomers as compared to **16d'**.

highly hindered nitrogen on the sterically blocked acid carbonyl becomes increasingly more problematic.

Of interest is the NMR of the product mixture in the 3,3-disubstituted **11d** systems which reveals the formation of a small amount of *trans*-bisimide **16d'** (see Figure 12). The relative amount of this isomer increases from 5% of the bisimide mixture to a value of 25% as the temperature continues to rise in subsequent thermal steps. The spectral data of each isomer is clearly discernible (see Experimental Section), and the $J_{1,2}$ for the *cis*-bisimide is 9.6 Hz, somewhat smaller than the 10.0 Hz splitting of the *trans* isomer. Surprisingly, the usually sensitive central C-13 methylenes of the two isomers overlap (at 4.029 ppm). Such isomerizations are well preceded at *ca.* 200 °C,^{35,36} and presumably proceeds via enol formation. *Ab initio* calculations (Gaussian 2009 using B3LYP/6-13G* basis set)³⁷ reveal that the *trans*-bisimide **16d'** is 1.7 kcal/mol more stable than the *cis* analogue **16d**. However, the intermediate ketoenol **20** (involving enolization of carbonyl at C-7) lies uphill by 26.12 kcal/mol. The alternate ketoenol **21** (formed via the enolization of carbonyl C-8) lies higher still at 26.73, while dienol **22** is totally out of reach at 42.32 kcal/mol.

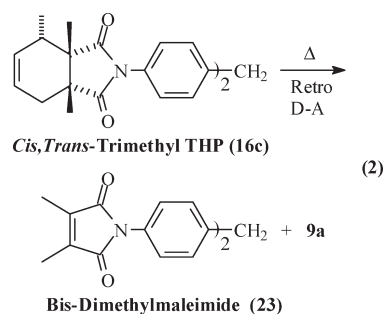
By comparison, Table 1 reveals that, after the first thermal step, the industry standard nadic anhydride (NA) is primarily converted to bisimide (79%), with the remaining end-cap present as the moniimide (5%) and monoimide monoamic acid (16%). By the second thermal step (*vide infra*) the latter are fully imidized.

(2). *Second Thermal Step.* Temperatures are raised in the second thermal step to 315 °C, and the relative amount of amic acids **14** and **15** drops, as they cyclize to the corresponding bisimide **16**; the relative percentage of the latter increases concomitantly. After this step, the bisimide is now the clearly predominant product from which the subsequent products are obtained. Bisimide represents 90% of the product obtained in both the unsubstituted THP system **11e** and the 2,3-disubstituted **11a**; 82% in the 3,3-disubstituted **11d** systems; but only 63% for the trisubstituted **11c**. As noted above, the relative amount of bisimide **16** is directly related to the amount of ring substitution.

It is important to emphasize that bisimide **16** should be viewed as a model PMR bisimide for which $n = 0$ (see Figure 1), i.e., incorporating only end-capped MDA and no BTDA. Analysis of the reaction products from here on will allow us to explore how the substitution pattern in the THP type systems affects the distribution and rate of formation of the remaining products. The observation that imidization of THP anhydrides **11** with MDA to bisimides **16** does not proceed to completion—even in the unsubstituted analogues—is the first complication in preparing thermally stable high temperature polyimides from this system. Nevertheless, longer hold times at intermediate temperatures or use of catalysts might drive the reaction to completion.

By comparison, Table 1 reveals that in the second thermal step of the nadic anhydride system, all the end-cap has undergone imidization and partial cross-linking.

(3). *Third Thermal Step.* In the third thermal step, after 50 min at 343 °C, the transformation of bisimide **16** into both cross-linked structure **18** is observable and to a much lesser extent to aromatized products (**17**, and perhaps **19**—*vide infra*). It is noteworthy that since model bisimide compounds **16** are of low molecular weight and yield cross-linked products of short chain-lengths, the resulting oligomers are completely CDCl₃ soluble. Figure 13 graphs the effect of temperature on the amount of cross-linking and aromatization. In most cases (**16a**, **c**, and **e**), cross-linking is low (5–9%) while aromatization is a mere 0–2%. Interestingly, in the case of trimethylated **16c**, an additional bisimide is observed (C₁₃-methylene at 3.996 ppm decreases as one at 4.006 ppm grows in) which has been identified as bis(dimethylmaleimide) **23** (see eq 2). The latter is presumably formed via a retro Diels–Alder process which is well-precedented in congested THP systems at 343 °C.⁸ In the case of **16c**, the congestion results from the adjacent *cis* and eclipsed methyl groups on C-1 and C-2. The loss of **9a** is evidenced by the sudden rise in the weight loss curve of **16c** at 343 °C (see Figure 10).



As compared to the sluggish thermolysis of **16a**, **c** and **e**, truly surprising is the exceptional reactivity of the

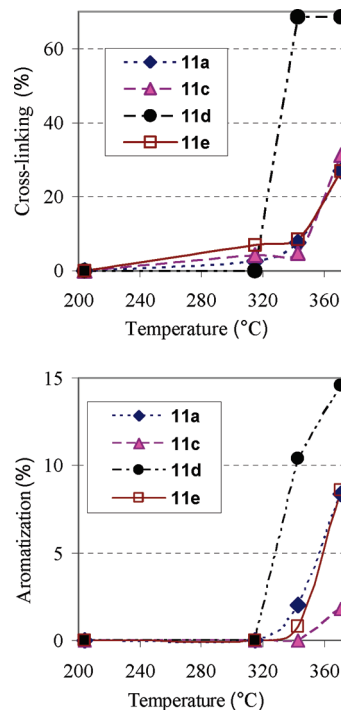
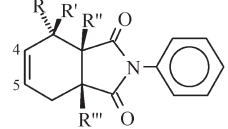
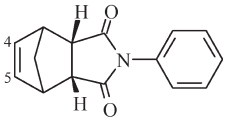


Figure 13. Percent cross-linking (above) and aromatization (below) in the air thermolysis of substituted bisimides **16** formed from 1:2 mixtures of MDA and anhydrides **11**.

Table 3. *Ab Initio* Calculated C₄–C₅ Double Bond Length of *N*-Phenyl Tetrahydrophthalimides **24** and *N*-Phenyl Nadimide **25**

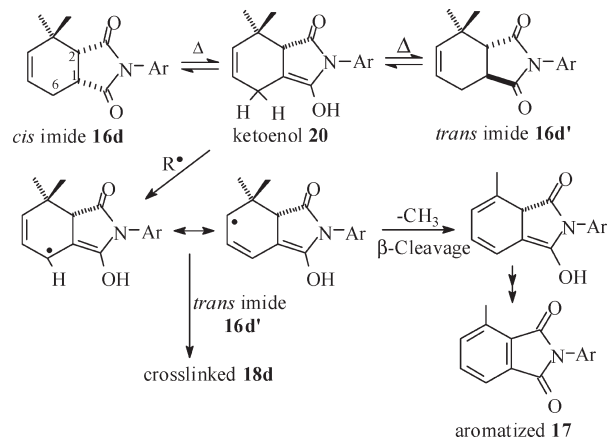
	
N-Phenyl THP-imide (24)	
a: R = R'' = CH ₃ ; R' = R''' = H	1.3356
c: R = R'' = R''' = CH ₃ ; R' = H	1.3321
d: R = R' = CH ₃ ; R'' = R''' = H (<i>cis</i>)	1.3357
d': R = R' = CH ₃ ; R'' = R''' = H (<i>trans</i>)	1.3404
e: R = R' = R'' = R''' = H	1.3345
	
N-Phenyl Nadimide (25)	
	1.3409

3,3-disubstituted system **16d**—which undergoes both extensive cross-linking (**18d**, 69%) and aromatization (**17d**, 10%) at this temperature. In order to understand this phenomenon, *ab initio* calculations (Gaussian 2009 using B3LYP/6-13G* basis set)³⁷ were used to determine the C₄–C₅ double bond length of the *N*-phenyl tetrahydrophthalimides **24a**, **c**, **d**, **d'**, and **e**, as well as that of the reactive *N*-phenyl nadimide **25**. We hypothesized that the longer the double bond length, the more reactive it would be toward cross-linking. Table 3 reveals that the C=C bond length of all the tetrahydrophthalimides **24** fell in the range of 1.3321–1.3357 Å, irrespective of substitution pattern. There was one exception, however, 3,3-dimethyl *trans*-imide **24d'**, whose double bond length was 1.3404 Å—substantially longer and nearly identical to the 1.3409 Å calculated for the highly reactive nadimide **25**.

These results suggest the scenario outlined in Figure 14. As the thermolysis temperature rises, *cis*-bisimide **16d** isomerizes to *trans*-bisimide **16d'** via ketoenol **20**. The C₄–C₅ double bond of **16d'** (like that of the nadic family) is substantially longer than the other analogues of **16** and undergoes more facile cross-linking. Also noteworthy in this regard is that in ketoenol **20** the C-6 methylene hydrogens are doubly allylic and particularly prone to radical abstraction. As outlined in Figure 14, this in turn encourages both cross-linking to **18d** and β -cleavage mediated aromatization to **17**. More will be said about the aromatization product in the next section.

By comparison, by the third thermal step, the industry standard nadic anhydride is fully cross-linked, and no aromatized product is detected.

(4). *Fourth Thermal Step.* In the fourth and final thermal step, the thermolysis temperature is raised to 371 °C for 30 min. The amount of bisimide decreases generating a concomitant amount of cross-linked oligomers **18** and aromatized product **17** (and/or **19**, *vide infra*). For systems **11a**, **d**, and **e**, the ratio of cross-linking to aromatization (**18**:**17**) is *ca.* 3. This aromatization occurs, despite the presence of methyl groups at junctions (C-1, C-2 and/or C-3) that should have blocked it. Obviously, at these elevated temperatures, oxidative cleavage of the pendant methyl groups allowing aromatization becomes more favorable. Here is further indication of the difficulty in preparing thermally stable high temperature polyimides from the THP system. Since the amount of aromatization competes effectively with cross-linking even in these methylated THP systems, the products obtained will be frangible—as has indeed been reported for the unsubstituted case.^{9,10}

**Figure 14.** Proposed mechanism for the facile cross-linking and aromatization of bisimide **16d**.

The only exception to the above observations is the 1,2,3-trimethyl system **11c**, where the ratio of cross-linking to aromatization (**18**:**17**) is *ca.* 17. Here, the angular methyls at both carbons C-1 and C-2 synergistically inhibit aromatization, though they do not prevent it completely. Nevertheless, as noted above, in this sterically congested system, imidization does not proceed to completion; even after 30 min at 371 °C, 23% of uncyclized amic acid remains.

There is one more comment that needs to be made about the yield of aromatization product. In the reactive **11d** system, after the third thermal step (343 °C) present system, 68.6% of the product was cross-linked **18d**, while 10.4% was aromatic product. Following the fourth thermal step, at 371 °C, the amount of aromatic product is up by 14.2% to 24.6%. At the same time, however, bisimide (**16d** + **16d'**) has decreased by only 4%, while the amount of cross-linked polymer **18d** has decreased by 10%. It is clear, therefore, that the increase of 14% in aromatic product comes in large part (presumably 10%) from the aromatization of the cross-linked polymer leading to cross-linked phthalimides **19**. (Indeed, a large singlet presumably corresponding to H₆ of **19** is observed at 7.262 ppm.) While this analysis is correct for the **11d** system, it is not required in the other systems—though there is no simple way of ruling it out. This is the reason that the aromatic product in Table 1 is designated as the sum of **17** + **19**.

Conclusion

Our previous study of the thermolysis THP end-capped polyimides, revealed that aromatization competes with cross-linking yielding a frangible product. In the present study, several THP end-caps were synthesized with one or more methyls placed strategically at the bridgehead C-1 and C-2 positions, and/or on the adjacent ring carbon C-3. Our hope was that upon imidization and thermolysis these critically placed methyl groups would inhibit aromatization and allow us entrée into a new class of thermally stable high temperature polymers. Indeed, in the 1,2,3-trimethylated analogue (**16c**), aromatization is kept below 2% of the product. Unfortunately, however, imidization with MDA is slowed by this very methylation. Interestingly, the pendant methyl groups are oxidatively cleaved at higher temperatures resulting in aromatization; the latter is indeed the preferred pathway for degradation after cross-linking.

Most surprising and promising is the behavior of 3,3-dimethyl THP (**16d**) which at 343 °C gives 70% cross-linking and 10% aromatic product. The secret to its surprising reactivity is presumably the facile isomerization of this *cis*-imide to *trans*-imide

(16d'). *Ab initio* calculations show that the latter is thermally more stable, though it contains a longer double bond equal in length to that of the nadic end-cap. These results would indicate that the reactivity of a double bond to cross-linking is correlated with its bond length.

The thermal properties, TOS and mechanical properties of PMR-type polyimides, prepared from MDA, BTDE and 3,3-dimethyl THP **11d** as the end-cap, are presently under investigation.

Acknowledgment. Thanks to Dr. Hugo E. Gottlieb for his expertise in NMR analysis and Dr. Pinchas Apeid for the Gaussian 2009 *ab initio* calculations. This paper is based in part on the Ph.D. Thesis of David Rajsfus, Bar Ilan University, September 2009.

Supporting Information Available: Text about and tables of the crystallographic data for compounds **11c** and **12a** and figures showing the X-ray structures of **11c** and **12a** and typical ^1H NMR spectra of the product mixture from the thermolysis of **16d**. This material is available free of charge via the Internet at <http://pubs.acs.org>.

References and Notes

- (1) Serafini, T. T.; Delvigs, P.; Lightsey, G. R. *J. Appl. Polym. Sci.* **1972**, *16*, 905–915.
- (2) Delvigs, P. *Polym. Compos.* **1989**, *10*, 134–139.
- (3) Meador, M. A. *Annu. Rev. Mater. Sci.* **1998**, *28*, 599–630.
- (4) Meador, M. A. B.; Johnston, J. C.; Cavano, P. J.; Frimer, A. A. *Macromolecules* **1997**, *30*, 3215–3223.
- (5) Meador, M. A. B.; Johnston, J. C.; Cavano, P. J. *Macromolecules* **1997**, *30*, 515–19.
- (6) Meador, M. A. B.; Lowell, C. E.; Cavano, P. J.; Herrera-Fierro, P. *High Perform. Polym.* **1996**, *8*, 363–379.
- (7) Meador, M. A. B.; Johnston, J. C.; Frimer, A. A.; Gilinsky-Sharon, P. *Macromolecules* **1999**, *32*, 5532–5538.
- (8) Meador, M. A. B.; Frimer, A. A.; Johnston, J. C. *Macromolecules* **2004**, *37*, 1289–1296.
- (9) Alston, W. B. Personal Communication, NASA Glenn Research Center: Cleveland, OH, August 16, 2002.
- (10) St. Clair, A. K.; St. Clair, T. L. *Polym. Eng. Sci.* **1982**, *22*, 9–14.
- (11) Frimer, A. A. "The Oxygenation of Enones. In *The Chemistry of Enones*, Part 2; Patai, S., Rappoport, Z., Eds.; Wiley: Chichester, U.K., 1989; pp 781–921.
- (12) Crowshaw, K.; Newstead, R. C.; Rogers, N. A. J. *Tetrahedron Lett.* **1964**, 2307–2311.
- (13) Howe, R.; McQuillin, F. J. *J. Chem. Soc.* **1958**, 1513–1518.
- (14) Buechi, G.; Pickenhagen, W.; Wuest, H. *J. Org. Chem.* **1972**, *37*, 4192–4193.
- (15) Hendry, D. G.; Schuetzle, D. *J. Am. Chem. Soc.* **1975**, *97*, 7123–7127.
- (16) Van Tamelen, E. E.; Hildahl, G. T. *J. Am. Chem. Soc.* **1956**, *78*, 4405–4412.
- (17) Gottlieb, H. E.; Kotlyar, V.; Nudelman, A. *J. Org. Chem.* **1997**, *62*, 7512–7515.
- (18) Brocksom, T. J.; Constantino, M. G. *J. Org. Chem.* **1982**, *47*, 3450–3453.
- (19) Gosselin, P.; Bourdy, C.; Mille, S.; Perrotin, A. *J. Org. Chem.* **1999**, *64*, 9557–9565.
- (20) Alemany, L. B.; Brown, S. H. *Energy Fuels* **1995**, *9*, 257–268.
- (21) Stokes, H. L.; Welker, M. E. *Organometallics* **1996**, *15*, 2624–2632.
- (22) Giri, R.; Yu, J.-Q. *J. Am. Chem. Soc.* **2008**, *130*, 14082–14083. See Supporting Information therein for compound 1f.
- (23) Inoue, S.; Shiola, H.; Fukumoto, Y.; Chatani, N. *J. Am. Chem. Soc.* **2009**, *131*, 6898–6899. See Supporting Information therein for compound 2j.
- (24) Hegazy, M.-E. F.; Shishodo, K.; Hirata, T. *Tetrahedron: Asym.* **2006**, *17*, 1859–1862.
- (25) Diels, O.; Alder, K. *Justus Liebigs Ann. Chem.* **1928**, *460*, 98–122.
- (26) The full X-ray analysis data is available in the Supporting Information.
- (27) March, J. *Advanced Organic Chemistry*, 4th Ed., New York: Wiley, 1992; p 842.
- (28) Houk, K. N. *J. Am. Chem. Soc.* **1973**, *95*, 4092–4094.
- (29) Houk, K. N.; Sims, J.; Duke, R. E., Jr.; Strozier, R. W.; George, J. K. *J. Am. Chem. Soc.* **1973**, *95*, 7287–7301.
- (30) Hoffmann, R.; Woodward, R. B. *Acc. Chem. Res.* **1968**, *1*, 17–22.
- (31) Woodward, R. B.; Katz, T. J. *Tetrahedron* **1959**, *5*, 70–89.
- (32) As already noted, the thermolysis of tetrahydrophthalic anhydride **11e** has been previously described by us.⁸ Although qualitatively the present results are essentially the same, the thermolysis in this case progressed more slowly. This discrepancy is attributable to a difference in the oven setup used. In the previous study, heating was carried out in a very large oven with forced air flow; the temperature was controlled from an average of a dozen thermocouples located at various positions around the oven. In the present study, a relatively small 6 L Carbolite ELF 11/6B oven with standing air was used; presumably the reaction vessel temperature in the latter case was cooler.
- (33) Milhourat-Hammadi, A.; Chayrigues, H.; Merienne, C.; Gaudemer, A. *J. Polym. Sci., Part A: Polym. Chem.* **1994**, *32*, 203–217.
- (34) Milhourat-Hammadi, A.; Gaudemer, F.; Merienne, C.; Gaudemer, A. *J. Polym. Sci., Part A: Polym. Chem.* **1994**, *32*, 1593–1597.
- (35) Nazarov, I. N.; Kuchero, V. F. *Russ. Chem. Bull.* **1952**, *1*, 301–307.
- (36) Nazarov, I. N.; Kuchero, V. F. *Russ. Chem. Bull.* **1954**, *3*, 269–275.
- (37) Gaussian 09, Revision A.02. J. Gaussian, Inc.: Wallingford, CT, 2009.